The ingap state spectral properties in the cuprates' pseudogap phase

Julius. Ranninger[1] and Alfonso. Romano[2]

[1]*Institut Néel, CNRS et Université Joseph Fourier, BP 166, 38042 Grenoble Cedex 09, France*
[2]*Laboratorio Regionale SuperMat, CNR-INFM, Baronissi (Salerno), Italy, and*
Dipartimento di Fisica "E. R. Caianiello", Università di Salerno, I-84081 Baronissi (Salerno), Italy

(Dated: March 23, 2010)

The single-particle excitations, which initiate the pseudogap in the cuprate superconductors at some temperature T^*, relate to specific local spectral features of resonant pairing, where charge carriers get momentarily trapped on dynamically deformable molecular Cu-O-Cu clusters. We show how those local excitations evolve into dispersive branches with a characteristic "S"-like shape for three-peak structured ingap excitations in the cuprates' pseudogap phase, when we consider a lattice of such clusters. This feature should be detectable in "momentum distribution curve" ARPES analysis.

PACS numbers: 74.20.-z,74.20.Mn,74.25.Jb

Introduction. Superconductivity in the cuprates evolves out of an insulating state of phase uncorrelated pairs of charge carriers, when doping beyond a certain concentration of $x_{sc} = 5 - 10\%$ holes per Cu ion. Alternatively, for $x \geq x_{sc}$, the superconducting state can be obtained out of the pseudogap state, which sets in below a certain $T^*(x)$. The opening of the pseudogap is due to phase uncorrelated fluctuating diamagnetic pairs. It is unrelated to any superconducting precursor pairing,[1] which sets in below a certain temperature $T_M(x) \leq T^*(x)$ where these bonding pairs acquire phase correlations on a finite space/time scale. This is evidenced in: a transient Meissner screening, the Nernst effect in thermal transport, torque magnetization measurements and zero bias conductance of pseudogap/superconducting junctions.[2] Our scenario of resonant pairing, attributed to the intrinsic metastability of the cuprate crystal structure, involves dynamically fluctuating molecular Cu-O-Cu clusters,[3–5] which, momentarily capture charge carriers in form of bound singlet pairs, respectively accommodate them as itinerant particles while passing through them. This causes a breaking of crystalline symmetry on a local level,[6] which makes the fermionic charge carriers to be partly itinerant and partly localized, as observed in STM imaging studies, see Ref.[7] and references therein. A duplicitous feature of fermionic charge carriers,[8] coexisting in localized and delocalized states, had been known for some time in dilute polaronic systems, in the region separating the anti-adiabatic and adiabatic regimes [9]. It was this dual localization-delocalization feature, which lead one of us (JR) to conjecture in the early eighties, that in a Many Body polaronic system, it should result in an intrinsic metastability of such compounds. It was a natural extension of the work on the Bipolaronic Superconductivity,[10] an extremely fragile state of matter, most likely unrealizable in real materials, which prefer to localize their charge carriers under similar conditions.[11]. In an attempt to materialize a superconducting state in strongly coupled electron lattice systems, it appeared judicious to consider the possibility of fluctuating bipolaronic states rather than bound states. This led to the proposition of a phenomenological model, the Boson Fermion model (BFM). A first attempt to explore this scenario [12] showed a pairing state below a certain temperature T^*, driven by a finite amplitude of the local pairing field. Such a state was later on ascribed to as the pseudogap state in the cuprates. Upon lowering the temperature this state can, but does not have to, condense into a phase correlated superfluid states. Depending on the concentration of charge carriers, it can equally result in an Mott correlation driven bipolaronic insulator. A prime motivation for introducing this scenario was the widely appreciated fact that metastable crystalline structures support fluctuating diamagnetic pairs, which favored a superconductivity that avoided the stringent limitations of phonon mediated low temperature BCS Cooper pairing.[13] and thus could attain substantially higher critical temperatures T_c,[14, 15]. The BFM, which captures the basic physics of polaronically driven pair fluctuating systems, can account for the emergence of a phase correlated superconducting state of locally fluctuating bipolarons out of their correlation driven Mott-like insulating state.[16] The Boson-Fermion exchange mechanism proposed in this model avoids the condensation into the Bipolaronic Superconductor state. It preserves the fermionic character of the system, albeit with a fractionated Fermi surface [6, 17] and controls the breakdown of the superconducting state at T_c by phase (i.e., via the disappearance of the density of superfuid carriers) rather than amplitude fluctuations.

The pair fluctuation driven pseudogap, predicted on the basis of this model, [19] manifests itself in a wide temperature regime above T_c. It exhibits ingap states, whose nature is considered to play a key role in our attempt to understand high T_c superconductivity. The single-particle spectral function $A(\mathbf{k}, \omega)$ in this pseudogap phase in the temperature regime $[T_M, T^*]$, is predominantly determined by the strong local phase correlations between

itinerant and localized pairs of charge carriers on individual clusters, which make up the effective lattice sites of these cuprates. We show here how this local physics, which is at the origin of duplicitous localized and delocalized charge carriers, is carried over into the spatial (alias momentum) dependent $A(\mathbf{k},\omega)$ and how the ingap states evolve into hybridized modes, constructed of (i) dispersionless branches, tracking the localized aspects and (ii) the bare tight binding spectrum of itinerant charge carriers, tracking their delocalized aspects.

The scenario. The BFM Hamiltonian, describing a lattice composed of effective sites which act as resonant trapping centers, is given by

$$H = \varepsilon_0 \sum_{i,\sigma} c^\dagger_{i\sigma} c_{i\sigma} - t \sum_{\langle ij\rangle,\sigma} c^\dagger_{i\sigma} c_{j\sigma} + E_0 \sum_i \rho^+_i \rho^-_i + g \sum_i [\rho^+_i c_{i\downarrow} c_{i\uparrow} + c^\dagger_{i\uparrow} c^\dagger_{i\downarrow} \rho^-_i]. \quad (1)$$

$c^{(\dagger)}_{i\sigma}$ denote the annihilation (creation) operators for fermions with spin σ at some effective sites i and ρ^+_i and ρ^-_i are pseudo-spin 1/2 operators, describing tightly bound fermion pairs which behave as hardcore bosons. t, g, $\varepsilon_0 = zt - \mu$, $E_0 = \Delta_B - 2\mu$ denote respectively: the hopping integral for the fermions, the boson-fermion pair-exchange coupling constant, the local fermion and boson energy levels with respect to the chemical potential μ, which has to be common to fermions and bosons, up to a factor 2 for the bosons being composed of two fermions. The bosonic and fermionic particles deriving from the same source, requires that at any given moment, such locally fluctuating bosonic pairs and itinerant unpaired fermionic charge carriers are in thermal equilibrium. A transition from a phase correlated superconducting into the phase uncorrelated insulating phase takes place for a boson concentration close to $n_B = 1/2$, when increasing g beyond a certain g_{SIT}. [16] We shall here consider that case, taking $n_{tot} = n_F + 2n_B = 2$ and study the cross-over at finite temperatures, from a metallic paramagnetic state into the diamagnetic pseudogap phase and eventually into a correlation driven insulator of phase uncorrelated pairs by gradually increasing g.

The prevailing physics of resonant pairing is related to the spectral properties of an isolated site, which is encoded in the spectral properties of the atomic limit of eq. 1, $H_{at} = lim_{t\to 0} H$. The Hilbert space of this local problem consist of eight configurations of product states made out of four fermionic states $|2\rangle = |c^\dagger_\uparrow\rangle$, $|3\rangle = |c^\dagger_\downarrow\rangle$, $|6\rangle = |c^\dagger_\uparrow \rho^+\rangle$, $|7\rangle = |c^\dagger_\downarrow \rho^+\rangle$ with energies $E_2 = E_3 = \varepsilon_0$, $E_6 = E_7 = \varepsilon_0 + E_0$ and four bosonic states $1\rangle = |0\rangle$, $|4\rangle \equiv |B\rangle = (1/\sqrt{2})[|c^\dagger_\uparrow c^\dagger_\downarrow\rangle - |\rho^+\rangle]$, $|5\rangle \equiv |AB\rangle = (1/\sqrt{2})[|c^\dagger_\uparrow c^\dagger_\downarrow\rangle + |\rho^+\rangle]$, $|8\rangle = |c^\dagger_\uparrow c^\dagger_\downarrow \rho^+\rangle$ with energies $E_1 = 0$, $E_B = -g$, $E_{AB} = +g$, $E_8 = 2\varepsilon_0 + E_0$. In order to keep the algebra as simple as possible, we shall restrict ourselves to the discussion of the case, where the bosonic level coincides with the center of the fermionic band i.e., $\Delta_B = 2\varepsilon_0$. This dictates the position of the chemical potential $\mu \simeq \Delta_B/2$ and implies a half-filled fermionic band ($n_F \simeq 1$). Putting $\varepsilon_0 = 0$, leads to $\Delta = \mu = 0$.

The single-particle Green's function for this atomic limit has been derived previously, [20, 21] and is:

$$G_{at}(i\omega_n) = -\int_0^\beta d\tau \exp^{i\omega_n \tau} \langle T[c_\sigma(\tau) c^\dagger_\sigma]\rangle = \frac{Z^F}{i\omega_n - \varepsilon_0} + \frac{1 - Z^F}{i\omega_n - \varepsilon_0 - g^2/(i\omega_n + \varepsilon_0 - E_0)} \quad (2)$$

with $Z^F = 2/(3 + cosh\beta g)$. This local single-particle spectral function $A_{at}(\omega) = -Im\, G_{at}(i\omega_n = \omega + i\delta)$ of an isolated cluster site is composed of two contributions: The first term arises from uncorrelated charge carriers. The second term is reminiscent of the single-particle spectral function for BCS superconductivity, with g playing the role of the gap. It describes the contributions coming from bonding $|B\rangle$, respectively anti-bonding states $|AB\rangle$. The significant difference between resonant pairing and BCS Cooper pairing is the appearance in the spectral function of temperature dependent spectral weights Z_F, respectively $1 - Z_F$. It monitors the relative weight of the intrinsic uncorrelated single-particle excitations and those which derive from bonding and antibonding pairing states, as we change g. We illustrate in Fig. 2 the variation with temperature of $A_{at}(\omega)$. As one reduces the temperature below a characteristic value $T \simeq g$, the spectral intensity of the single-particle non-bonding excitations Z^F at $\omega = 0$, shows a significant drop and goes to zero for $T \to 0$, while that of the bonding and antibonding states at $\omega = \mp g$ increases correspondingly. Simultaneously the local exchange correlations, given by $\langle c_\downarrow c_\uparrow \rho^+\rangle = (1/2) tanh(\beta g/2)$, show a marked increase upon decreasing T below g and saturates at 0.5 for $T \to 0$ (see Fig 3 in Ref. 21). These features indicate that the local density of states at the chemical potential ($\omega = 0$) rapidly drops below $T = g$. Considering a finite system, it forshadows the opening of a gap-like structure at the Fermi surface, which is independent of any symmetry breaking. We shall now explore, how this local physics, given by $A_{at}(\omega)$, evolves into dispersive modes, when putting such effective sites into a lattice with charge exchange between adjacent sites. Such questions have to be handled in a non-perturbartive scheme, because of the strong inter-relation between single and two-particle excitations in resonant pairing systems. We choose for that purpose a dynamical mean field theory (DMFT) analysis.

Single-particle spectral features. Taking into account the physics of the local problem (H_{at}) exactly, we reformulate the Hamiltonian, Eq. 1, for the D_∞ problem in the standard way by coupling this local physics, contained in H_{at} and discussed above, to a Weiss field, which mimics the itinerancy of the original fermions $c^{(\dagger)}_{i,\sigma}$ on a

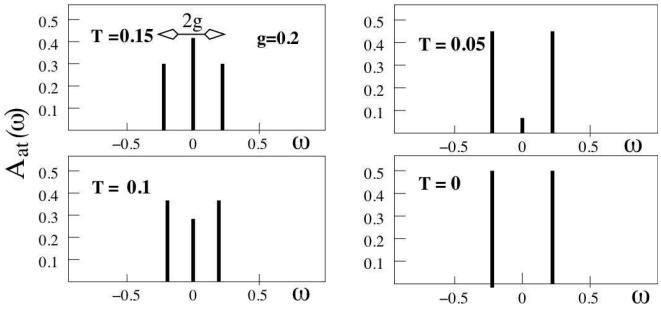

FIG. 1: The single-particle spectral function in the atomic limit as a function of frequency for different temperatures T.

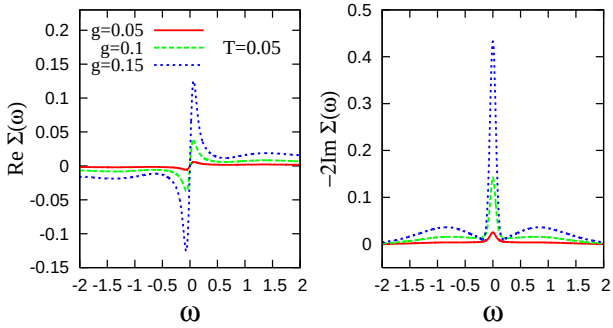

FIG. 2: (Color Online) Real and imaginary part of the fermionic self energy as a function of frequency ω for various values of g and $T = 0.05$ in units of D.

Bethe lattice. The effective Hamiltonian for that is

$$H = g\,[\,c^\dagger_\uparrow c^\dagger_\downarrow \rho^- + \rho^+ c_\downarrow c_\uparrow] + \sum_{k,\sigma} w_k d^\dagger_{k,\sigma} d_{k,\sigma} + \sum_{k,\sigma} v_k\,[\,d^\dagger_{k,\sigma} c_\sigma + c^\dagger_\sigma d_{k,\sigma}\,]. \quad (3)$$

$d^{(\dagger)}_{k,\sigma}$ denote the operators of the auxiliary Fermionic excitations of this Weiss field, having energies w_k and which are coupled to the original fermionic excitations on an "Anderson impurity" site by a hybridization term of strength v_k. After rewriting this Hamiltonian in terms of Hubbard operators, corresponding to H_{at} of the isolated local problem, we calculate the local Green's function $G_{imp}(i\omega_n) = [i\omega_n - \varepsilon_0 - \Sigma_W(i\omega_n) - \tilde{\Sigma}^g_{int}(i\omega_n)]^{-1}$. Requiring $G_{imp}(i\omega_n)$ to be identical to the local part of lattice Green's function $G_{lat}(i\omega_n) = \int d\varepsilon\,\rho(\varepsilon)[i\omega_n - \varepsilon - \widetilde{\Sigma}^g_{int}(i\omega_n)]^{-1}$, we obtain $\Sigma_W(i\omega_n) = t^2 G_{imp}(i\omega_n)$, which determines the spectral distribution of the Weiss field energies $\{w_k\}$ in a selfconsistent way. $\rho(\varepsilon) = (1/2\pi t^2)\sqrt{\varepsilon(4t-\varepsilon)}$ denotes the density of states of bare uncoupled fermions of the lattice problem in D_∞ with a band width $D = 4t$. Once having obtained $\Sigma_W(i\omega_n)$, we deduce the selfenergy for the lattice problem via $\tilde{\Sigma}^g_{int}(i\omega_n) = i\omega_n - \Sigma_W(i\omega_n) - [G_{imp}(i\omega_n)]^{-1}$. In determining $G_{imp}(i\omega_n)$, we use a modification of the original Non-Crossing Approximation (NCA) approach by Bickers [22], adapted to the present BFM in Ref.[23]. By introducing $\widetilde{\Sigma}^g_{int}(i\omega_n) \equiv \Sigma^g_{int}(i\omega_n) - \Sigma^{g=0}_{int}(i\omega_n)$ we subtract out the effect of kinematic interactions, which arise in such a NCA formalism and are able in this way to describe qualitatively correctly the redistribution of spectral weight of the fermionic excitations over the entire frequency regime of the fermionic excitations. We illustrate in Fig. 2 the real and imaginary part of the fermionic selfenergy for a given temperature $T = 0.05$ and for three characteristic values of g, which describe the (i) a paramagnetic metallic phase for $0.05 < g < 0.1$ and (ii) the pseudogap phase of diamagnetic bonding pairs, merging into a correlation driven insulator for $0.1 < g < 0.15$. The onset of the pseudogap phase is manifest in the single-particle excitations, by the abrupt appearence above $g = 0.1$ of a three-pole structure of the lattice Green's function, given by $i\omega - \varepsilon - Re\widetilde{\Sigma}^g_{int}(i\omega) = 0$. This is illustrated in Fig. 3, where we plot the real (ω^*) and imaginary ($Im\Sigma(\omega^*)$ parts of these poles. Upon approaching $g = 0.1$ from below, ω^* as a function of the bare fermionic spectrum $\varepsilon_{\mathbf{k}} = -tcos\mathbf{k}$ (presented here by its corresponding energy ε, develops a kink-like structure around the chemical potential at $\varepsilon = 0$ and finishes up in a vertical slope upon approaching $g = 0.1$ $T = 0.05$. With further increasing g, we find in a restricted region of momentum (alias ε) around $\varepsilon = 0$, simultaneously three dispersing modes. Two of them, the red continuous line and the blue dotted line outside the pseudogap, follow qualitatively the unrenormalized bare dispersion $\varepsilon_k \equiv \varepsilon$. Inside the pseudogap however, the renormalization turns the non-bonding states into a characteristic S-like shape (the green dashed line) in accordance with the three-pole structure of the atomic limit of the local spectral properties of $A(\omega)_{at}$. This S-like dispersing single-particle feature is a finger print of resonant pairing which unlike in the socalled cross-over scenario results not simply in bound pairs but in strongly locally phase correlated localized and delocalized states of bonding and anti-bonding states $|B\rangle$ and $|AB\rangle$. Following the socalled Fermi-arcs in the Brillouin zone of the cuprate CuO_2 planar electronic structure, going from the nodal toward the anti-nodal point, whereupon the effective g increases, the changeover from a well defined single ingap dispersive branch $\omega^*(\varepsilon) \simeq \varepsilon$ to an overdamped one dispersing in the S like shape discussed above, should be clearly visible in a "momentum distribution curve" ARPES analysis. We plot it for that purpose in Fig. 4 for a set of equidistant energies ω, concentrating on the pseudogap energy region. Identifying the peak positions of the various curves, corresponding to different ω's, with the corresponding values of ε we deduce the dispersion of those ingap excitations, which, as it should be, coincide with the dispersion of $\omega^*(\varepsilon)$ (see Fig. 3).

Discussion On the basis of a resonant pairing scenario and the Boson-Fermion model, where charge carriers are partly in localized pairing states and partly in

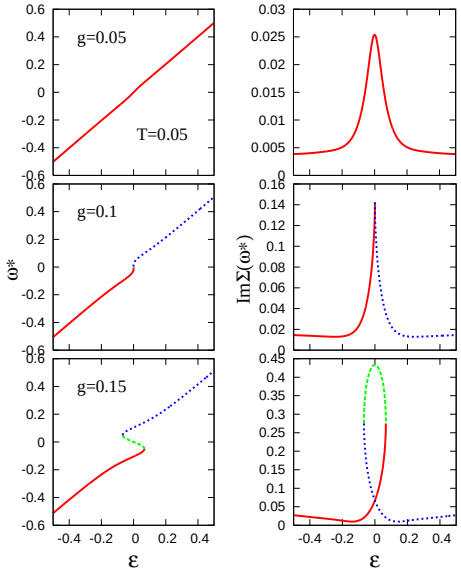

FIG. 3: (Color Online) The real and imaginary parts of the poles of the single-particle Green's functions as a function of the bare energies ε of the fermionic particles, measured from the chemical potential and for a given temperature $T = 0.05$ and different values of g in units of D.

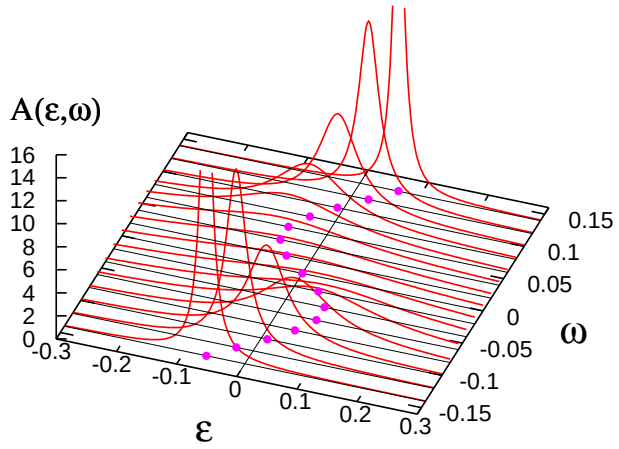

FIG. 4: (Color Online) The single-particle spectral function $A(\varepsilon, \omega)$ as a function of the bare electron dispersion ε, scanning the various energies inside the pseudogap.

delocalized single-particle states, we illustrated how the local physics of such systems, derived from their intrinsic metastability, evolves into diffusive dispersing ingap states in the pseudogap phase of the cuprates. Such modes never appear as well defined single-particle modes in such a resonant pairing scenario, in clear distinction to any BCS like physics [24]. They are intrinsically overdamped, with a width extending over the entire pseudogap frequency region. Nevertheless, we can distinguish a characteristic S-like dispersion, which is imposed by the underlying local physics and which dictates the features of dispersing excitations. This is illustrated in presenting the single-particle spectral function $A(\mathbf{k}, \omega)$ as a function of momentum $\mathbf{k}$ and scanning the energies inside the pseudogap. Experimentally it should be possible to verify this by examining the "momentum distribution curves" of ARPES experiments and by going across the hidden Fermi surface near the antinodal points. In the present study we considered a temperature regime below the onset of the pseudogap at T^*, where fluctuating diamagnetic pairs on molecular clusters are spontaneously created and destroyed. These ingap states are best seen in this temperature regime, since below T_M the onset of spatial superconducting phase correlations between the local diamagnetic fluctuations will strongly diminish the spectral intensity of those ingap states, having shifted their spectral weight to emerging diffusive Bogoliubov branches.

Acknowledgement We thank Tadek Domanski for numerous discussions and comments on the manuscript.

[1] A. N. Pasupathy et al., Science **320** 196 (2008).
[2] J. Corson et al., Nature (London) **398**, 221 (1999);Z. A. Xu et al., Nature **406**, 486 (2000); L. Li et al., Phys. Rev. B **81**; 054510 (2010); N. Bergeal et al., Nature Physics **4**, 608 (2008).
[3] J. Ranninger and A. Romano, Phys. Rev. B **78**, 054527 (2008).
[4] J. Ranninger, cond.mat: 1001.2143vl (2010).
[5] J. Ranninger and T. Domanski, Phys. Rev. B **81**, 014514 (2010).
[6] Y. Kohsaka et al., Nature **454**, 1072 (2008).
[7] J. Lee et al., Science **325**, 1099 (2009).
[8] T. Hanaguri, Nature **454**, 1062 (2008).
[9] D. M. Eagles, Phys. Status Solidi B **48**, 407 (1971); K. Cho and Y. J. Toyozawa, Phys. Soc. Jap., **30**, 1555 (1971); H. B. Shore and L. M. Sanders Phys. Rev. B **7**, 4537 (1973).
[10] A. S. Alexandrov and J. Ranninger, Phys. Rev. B **23**,1796 (1981).
[11] B. K. Chakraverty, J. Ranninger and D. Feinberg, Phys. Rev. Lett. **81**,433 (1998).
[12] J. Ranninger and S. Robaszkiewicz, Physica B **135**, 468 (1985).
[13] P. W. Anderson and B. T. Matthias, Science **144**, 373 (1974).
[14] J. M. Vandenberg and B. T. Matthias, Science **198**, 194 (1977).
[15] A. W. Sleight, Physics Today, **44**(6), 24 (1991).
[16] M. Cuoco and J. Ranninger, Phys. Rev. B **74**, 094511 (2006).
[17] W. S. Lee et al., Nature **450**, 81 (2007).
[18] J. Ranninger in "Polarons in Bulk materials and systems with reduced dimensionality", Proceedings of International School of Physics "Enrico Fermi", Course CLXI, edited by G. Iadonisi, J. Ranninger and G. de Filippis (IOS Press, Amsterdam, 2006) p 327.
[19] J. Ranninger, J. M. Robin and M. Eschrig, Phys. Rev. Lett. **74**, 4027 (1995).
[20] T. Domanski, J. Ranninger and J. M. Robin, Solid State

Commun. **105**, 473 (1998).
[21] T. Domanski, Eur. Phys. J. B **33**, 41 (2003).
[22] N.E. Bickers, Rev. Mod. Phys. **59**, 845 (1987).
[23] A. Romano and J. Ranninger , Phys. Rev. B **62**, 4066 (2000).
[24] T. Senthil and P. A. Lee, Phys. Rev. Lett., **103**, 076402 (2009); . Senthil and P. A. Lee, Phys. Rev. B **79**, 245116 (2009).